Journal of Magnetic Resonance **147,** 357–360 (2000)
doi:10.1006/jmre.2000.2221, available online at http://www.idealibrary.com on IDEAL®

Determination of Internucleotide $^{h}J_{HN}$ Couplings by the Modified 2D J_{NN}-Correlated [^{15}N, ^{1}H] TROSY

Xianzhong Yan, Xiangming Kong, Youlin Xia, Kong Hung Sze, and Guang Zhu[1]

Department of Biochemistry, Hong Kong University of Science and Technology, Clear Water Bay, Kowloon, Hong Kong, SAR, People's Republic of China

Received May 1, 2000; revised August 30, 2000

Recent developments in the direct observation of *J* couplings across hydrogen bonds in proteins and nucleic acids provide additional information for structure and function studies of these molecules by NMR spectroscopy. A J_{NN}-correlated [^{15}N, ^{1}H] TROSY experiment proposed by Pervushin *et al.* (*Proc. Natl. Acad. Sci. USA* 95, 14147–14151, 1998) can be applied to measure $^{h}J_{HN}$ in smaller nucleic acids in an E.COSY manner. However, it cannot be effectively applied to large nucleic acids, such as tRNA^{Trp}, since one of the peaks corresponding to a fast relaxing component will be too weak to be observed in the spectra of large molecules. In this Communication, we proposed a modified J_{NN}-correlated [^{15}N, ^{1}H] TROSY experiment which enables direct measurement of $^{h}J_{HN}$ in large nucleic acids. © 2000 Academic Press

Key Words: **hydrogen bond; tRNA; NMR; TROSY; J_{NN}-correlated [^{15}N, ^{1}H] TROSY.**

Recently, several remarkable works have been published reporting the observation of scalar couplings between the hydrogen bond donating and accepting ^{15}N nuclei in Watson–Crick base pairs of ^{15}N-labeled double-stranded RNA (*1*) and DNA, and the smaller *J* coupling between the imino proton and the hydrogen bond accepting ^{15}N nucleus (*2*). Similar couplings were also found in Hoogsteen base pairs of RNA (*3*) and mismatched base pairs of DNA involving amino groups (*4, 5*). These observations provide unambiguous evidence of the existence of hydrogen bonds within these base pairs. This will be of great importance for the structure determination of nucleic acids, for which fewer protons than in proteins are available to obtain the NOE information for structure determination. In large biomolecules, due to the interference between dipole–dipole coupling and chemical shift anisotropy, the transverse relaxation rates are very different for each component of the multiplet in a system of two coupled $\frac{1}{2}$ spins, such as the imino group ^{15}N–^{1}H in nucleic acid. This results in different linewidths and peak intensities (*6, 7*). The component with the slowest transverse relaxation rate has been utilized in TROSY-based experiments (*8, 9*). The J_{NN}-correlated [^{15}N, ^{1}H] TROSY (*2*) experiment for the correlation of hydrogen-bonded nuclei and measurement of $^{2h}J_{NN}$ utilized the TROSY effect and thus is suitable for large molecules. However, the measurement of $^{h}J_{HN}$ by E.COSY type peaks in this experiment (*2*) is not practical for large molecules, such as tRNA, in which the fast-relaxing component is too weak to be detected, due to the significant loss of magnetization caused by relaxation during the long magnetization transfer delay of $4T$ and t_1 evolution time. Another method proposed by Dingley *et al.* (*10*) for the measurement of $^{h}J_{HN}$ based on the HSQC-type experiment is not suitable for large molecules. A novel method, $^{h}J_{HN}$-quantative [^{15}N, ^{1}H] ZQ TROSY, in which only the narrowest component of the ^{15}N–^{1}H multiplets was used, was reported recently to measure the $^{h}J_{HN}$ values in a 17-kDa protein–DNA complex (*11*). This method involves $^{h}J_{HN}$ modulating ^{1}H transverse magnetization before detection. Because smaller $^{h}J_{HN}$, compared to $^{2h}J_{NN}$, introduces a longer delay for magnetization modulation and the transverse relaxation of proton is faster than that of ^{15}N, this experiment may not be as sensitive as the J_{NN}-correlated [^{15}N, ^{1}H] TROSY experiment. Here we propose a modified J_{NN}-correlated [^{15}N, ^{1}H] TROSY (*2*) for measurement of the $^{h}J_{HN}$ coupling constant of large biomolecules and apply it to tRNA^{Trp}. In this experiment, only the slow-relaxing component is utilized during the long delay of $4T$ for both peaks used for $^{h}J_{HN}$ measurement, by using a method similar to that reported by Meissner and Sørenson (*12*). The appearances of the subspectra are similar to that of the doublet-separated HSQC experiment for the directly bonded NH group (*13*).

The J_{NN}-correlated [^{15}N, ^{1}H] TROSY (*2*) pulse sequence in Fig. 1A is modified for measuring $^{h}J_{NN}$, as depicted in Fig. 1B. Two data sets are recorded in an interleaved manner, with two pairs of 90° pulses flanking the t_1 evolution period. The phases of the two 90° pulses within each pair are opposite in the first experiment and the same in the second experiment. Only one component is selected in each experiment. With this arrangement, the first experiment is equal to the original J_{NN} HNN-COSY experiment (*1*). The slow-relaxing component is selected and the real part of the

[1] To whom correspondence should be addressed. Fax: 852-2358-1552. E-mail: gzhu@ust.hk.

1090-7807/00 $35.00

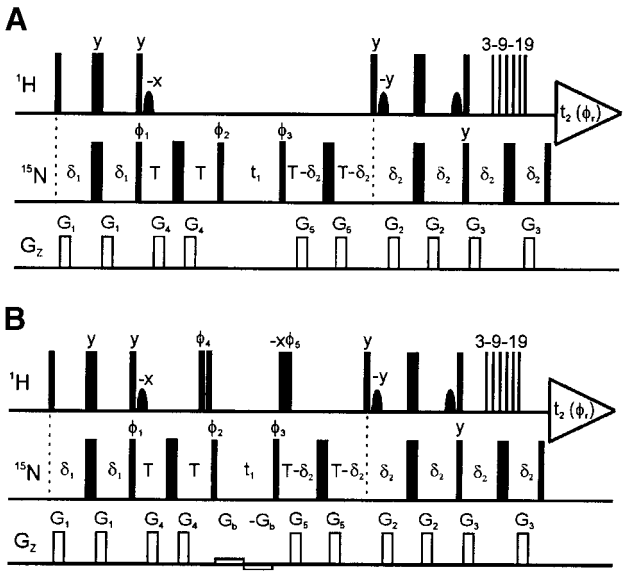

FIG. 1. Pulse sequences used in this paper for the measurement of $^{h}J_{HN}$. In all sequences, narrow and wide bars represent 90° and 180° pulses, respectively. Shaped pulses for the selectively excitation of water resonance are 1.7-ms sinc 90° pulses. Default phases are x. $\delta_1 = 2.25$ ms, $\delta_2 = 2.7$ ms, $T = 15$ ms. A 3–9–19 composite pulse was used for water suppression. Relaxation recovery delay is 1.0 s. The durations and strengths of the gradients along the z-axis are $G_1 = (0.4$ ms, 5 G/cm); $G_2 = (0.4$ ms, 8 G/cm); $G_3 = (0.4$ ms, 5 G/cm); $G_4 = (0.4$ ms, 10 G/cm); $G_5 = (0.5$ ms, 5 G/cm); G_b are 0.2-G bipolar gradients. Quadrature detection in t_1 for all experiments is achieved through altering ϕ_1 and ϕ_2 in a States–TPPI manner. (A) The E.COSY-type $^{h}J_{NN}$-correlation [^{15}N, ^{1}H] TROSY is similar to that reported by Pervushin *et al.* (*2*), except that only one experiment is carried out to observe both components with the same phase. The phase cycling is $\phi 1 = y, -y$; $\phi 2 = -x, -x, x, x$; $\phi_3 = 4(-x), 4(x)$; $\phi_r = y, -y$. (B) Modified $^{h}J_{NN}$-correlation [^{15}N, ^{1}H] TROSY. Two data sets are measured in an interleaved manner with the following phase cycling schemes: (I) $\phi_1 = x, y, -x, -y$; $\phi_2 = y, -x, -y, x, -y, x, y, -x$; $\phi_3 = -y, x, y, -x, -y, x, y, -x, y, -x, -y, x, y, -x, -y, x$; $\phi_4 = -x$; $\phi_5 = x$; $\phi_r = x, y, -x, -y$. (II) $\phi_4 = x$; $\phi_5 = -x$, while the other phases are the same as in (I). The resulting two spectra after Fourier transformation display cross peaks displaced along $\omega 1$ by proton–nitrogen coupling constants, $^{1}J_{HN}$ and $^{h}J_{HN}$, for direct and relayed correlation cross peaks, respectively.

detectable magnetization in the ω_1 dimension is of the following form,

$$S_r(I) = \frac{1}{2}(u + v)\{\cos^2(2\pi^{2h}J_{NN}T)\cos[(\omega_N + \pi^1 J_{HN})t_1] \times e^{-(R_2^N-\eta)4T}e^{-(R_2^N-\eta)t_1} + \sin^2(2\pi^{2h}J_{NN}T) \times \cos[(\omega_{N'} + \pi^h J_{HN})t_1]e^{-(R_2^N-\eta)4T}e^{-R_2^{N'}t_1}\} \times e^{i(\omega_H - \pi^1 J_{HN})t_2}e^{-(R_2^H-\eta)t_2},$$

where u and v are the relative magnitudes for the ^{1}H and ^{15}N steady-state magnetizations; R_2^N, $R_2^{N'}$, and R_2^H are the average transverse relaxation rates of H-bond donating N, accepting N′, and imino proton, respectively; and η is the relaxation rate due to the interference between dipole–dipole interaction and ^{15}N chemical shift anisotropy (CSA) interaction (*7*). The detectable magnetization described above is the resonance component with the slowest transverse relaxation in the $4T$, t_1, and t_2 periods. The proton donating and accepting ^{15}N nuclei have the chemical shifts of $\omega_N + \pi^1 J_{HN}$ and $\omega_{N'} + \pi^h J_{HN}$ in the ω_1 dimension, respectively.

In the second experiment, the proton spin state is exchanged just before and after the t_1 evolution period. Supposing that the transverse relaxation rate of spin N′ does not vary with the change of the proton spin state, the real part of the detectable signal in the ω_1 dimension is,

$$S_r(II) = \frac{1}{2}(u + v)\{\cos^2(2\pi^{2h}J_{NN}T)\cos[(\omega_N - \pi^1 J_{HN})t_1] \times e^{-(R_2^N-\eta)4T}e^{-(R_2^N+\eta)t_1} + \sin^2(2\pi^{2h}J_{NN}T) \times \cos[(\omega_{N'} - \pi^h J_{HN})t_1]e^{-(R_2^N-\eta)4T}e^{-R_2^{N'}t_1}\} \times e^{i(\omega_H - \pi^1 J_{HN})t_2}e^{-(R_2^H-\eta)t_2}.$$

The slow-relaxing nitrogen component is changed to the fast-relaxing component only during t_1 evolution, and the frequencies of proton donating and accepting ^{15}N spins are labeled with chemical shifts of $\omega_N - \pi^1 J_{HN}$ and $\omega_{N'} - \pi^h J_{HN}$ in the ω_1 dimension, respectively. This component is then changed back to the slow-relaxing component by the second pair of 90° pulses after t_1 and is then selected during acquisition as in the first experiment. The TROSY effect is present in the periods of $4T$ and t_2. For the diagonal peak, which corresponds to the first term in the above expression, the TROSY effect is not utilized in the t_1 period, but this is not our main concern. For the cross peak, which corresponds to the second term of the above expression, this experiment gives identical intensity to that in $S_r(I)$.

Consequently, in the nitrogen dimension, the fast-relaxing component evolves only in the t_1 period but with the slow-relaxing component employed during the long magnetization transfer delay of $4T$. In the proton dimension, the slow-relaxing component is recorded in both experiments. The difference between the peak intensities of these two experiments is introduced only by the different relaxation rates of the magnetization during the t_1 period. The steady-state enhancements are maintained and contribute to the peak intensity equally in both experiments (*14*).

In the second experiment, the water magnetization is put to the $-z$ direction during the t_1 interval. In order to avoid the recovery of the water magnetization from $-z$ due to radiation damping, a pair of bipolar gradient pulses is used. It has been shown that a weak gradient can effectively suppress the radiation damping effect (*15*). Also, the phases of the second pair of proton 90° pulses at the end of the t_1 interval are set to be

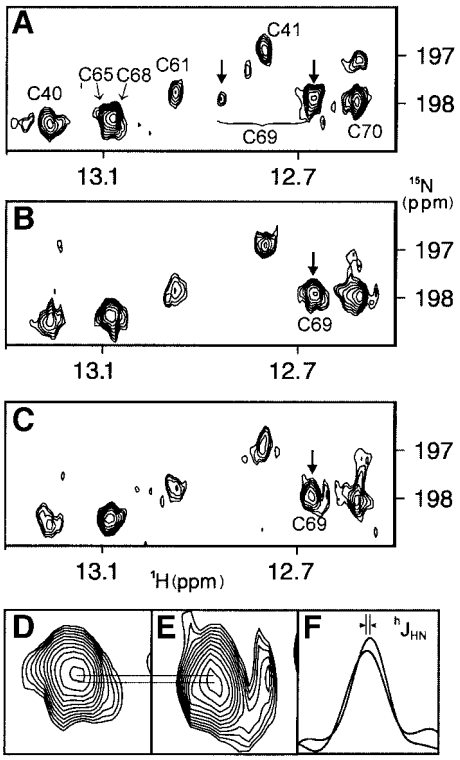

FIG. 2. Comparison of the measurement of $^{h}J_{HN}$ couplings using (A) E.COSY-type $^{h}J_{NN}$-correlation [^{15}N, ^{1}H] TROSY and (B, C) modified $^{h}J_{NN}$-correlation [^{15}N, ^{1}H] TROSY. Shown here are the GC base pair region spectra of the *B. subtilis* tRNA^{Trp} A73 mutant. (D, E) Enlargement of the cross peak of the G4C69 pair from (B) and (C), respectively. (F) Traces along $\omega 1$ taken from (D) and (E), with the difference of the peak position between two slices giving the $^{h}J_{HN}$ value. The spectra were acquired on a 500-MHz spectrometer with spectral widths and complex data points of 2027 Hz, 128 for $\omega 1$, and 12000 Hz, 2048 for $\omega 2$, respectively. The total acquisition time for each experiment is about 23 h.

opposite to the phases of the first pair of 90° pulses to compensate for an incomplete conversion of water magnetization to $+z$ resulting from the imperfection of pulse widths. A shorter 3–9–19 composite pulse instead of long soft selective pulses was used in the watergate sequence (*16*) to obtain better sensitivity for nucleic acids.

In the original 2D $^{h}J_{NN}$-correlation [^{15}N, ^{1}H] TROSY experiment (*2*), two data sets were recorded and after the addition and subtraction of these data sets, two subspectra were obtained. The peaks in one spectrum correspond to the components with the slowest transverse relaxation rate, and the peaks in the other correspond to those with the fastest transverse relaxation rate. Therefore, the ratio of diagonal peak intensities in the two spectra is proportional to $e^{(8\eta T)}(R_2^N + \eta)/(R_2^N - \eta)$, in which $e^{8\eta T}$ is approximately 7–8 at 25°C for a 69-nucleotide RNA domain (*1*). Since this ratio is very large, the spectrum corresponding to the fastest transverse relaxation component will be very weak. Accurate measurement of $^{h}J_{HN}$ will become impossible when this experiment is applied to large DNA or tRNA. In contrast, the resonant peaks in the two spectra that are obtained by the modified $^{h}J_{NN}$-correlation [^{15}N, ^{1}H] TROSY experiments proposed here will have comparable intensities for the $^{h}J_{HN}$ measurement of tRNA^{Trp}.

This approach is applied to the $^{h}J_{HN}$ measurement between hydrogen-bonded base pairs in *Bacillus subtilis* ^{15}N-labeled tRNA^{Trp} A73 mutant, of which the hydrogen-bonded imino groups have been completely assigned (*17*). tRNA is an L-shaped macromolecule with a molecular weight greater than 25 kDa. It has a long correlation time and broad linewidths in the NMR spectra, corresponding to a globular protein with a much larger molecular weight than 25 kDa (*6*). All spectra were recorded with peaks folded in f_1 to enhance the resolution without phase distortion (*18, 19*). The spectrum acquired by using the pulse sequence depicted in Fig. 1A is shown in Fig. 2A. The experiment in Fig. 1A is similar to the original $^{h}J_{NN}$-correlation [^{15}N, ^{1}H] TROSY (*2*), but with two component peaks in one spectrum for simplicity. In Fig. 2A, both the fast- and the slow-relaxing components used for $^{h}J_{HN}$ measurement exhibit very different peak intensities and linewidths due to the different transverse relaxation rates. As a result, only one pair of peaks is clearly observable in the GC pair region as indicated in Fig. 2A. Figures 2B and 2C show the results obtained with our modified $^{h}J_{NN}$-correlation [^{15}N, ^{1}H] TROSY experiment (Fig. 1B) by using the pulse sequence depicted in Fig. 1B. The measurements of $^{h}J_{HN}$ from peaks taken from Figs. 2B and 2C are shown in Figs. 2D–2F. Almost all cross peaks were observed in these spectra. The $^{h}J_{HN}$ coupling constants shown in Table 1 were calculated by reverse Fourier transformation of the slices corresponding to each peak along $\omega 1$, zero filling, and then Fourier transformation and data fitting. Although the cross peaks for G5C68 and G49C65 were strong, accurate $^{h}J_{HN}$ values could not be obtained due to peak overlap. Some other $^{h}J_{HN}$ values were also not available because of low peak intensities. The results show that the ap-

TABLE 1
$^{h}J_{HN}$ Coupling Constants of *B. subtilis* tRNA^{Trp} A73 Mutant

Base pairs	$^{h}J_{HN}$ (Hz)
U11A24	3.6
s^{4}U8A14	2.9
T54A58	2.5
G30C40	0.5
G53C61	1.0
A15U48	2.7
G29C41	2.7
U12A23	2.6
G4C69	1.8
G2C71	2.4
G52C62	2.6
G3C70	2.1
G10C25	2.8

proach we proposed here is a better way to measure the $^{h}J_{HN}$ coupling constants of base pairs in tRNA and other large nucleic acid molecules.

It should be pointed out that the intensities of the relayed cross peaks acquired on a 500-MHz spectrometer are much stronger than those acquired on a 750-MHz spectrometer (data not shown). The CSA of cytosine N3 in GC pairs and adenosine N1 in AU pairs is much larger than that of their corresponding proton donor nitrogen nuclei (*1, 20*), while the distance between these nitrogen nuclei and protons is about twice that between imino nitrogen and protons. This may result in the transverse relaxation of the proton accepting ^{15}N nucleus being dominated by CSA. Therefore, lower static magnetic field strength is thus favorable for the relayed cross peaks.

In conclusion, we have described a modified $^{h}J_{NN}$-correlation [^{15}N, ^{1}H] TROSY experiment to measure the $^{h}J_{HN}$ constants between a hydrogen-bonded proton and its accepting ^{15}N nucleus in RNA with large molecular weight. The slow-relaxing component is used during the long magnetization transfer delay and detection, resulting in optimized sensitivity and almost identical peak intensities for the two peaks labeled with frequencies $\omega_A + \pi^{h}J_{HN}$ and $\omega_A - \pi^{h}J_{HN}$ in the f_1 dimension. It has been shown that in proteins the J coupling across the hydrogen bond can be correlated to the length of the H-bond, which can provide distance constraints for the structure determination of proteins (*21*). An accurate measurement of $^{1h}J_{HN}$ and $^{2h}J_{NN}$ is essential for the application of a similar correlation to nucleic acids. The modified $^{h}J_{NN}$-correlation [^{15}N, ^{1}H] TROSY experiment can be readily applied to RNA and DNA with large molecular weight to facilitate the study of their structures and hydrogen bonds.

ACKNOWLEDGMENTS

This work is supported by grants from the Research Grant Council of Hong Kong (HKUST6197/97M, HKUST6038/98M, and HKUST6199/99M). The Hong Kong Biotechnology Research Institute is acknowledged for the purchase of the 750-MHz NMR spectrometer. The authors also thank Dr. H. Xue and Prof. J. Wong for their help with sample preparation.

REFERENCES

1. A. J. Dingley and S. Grzesiek, *J. Am. Chem. Soc.* **26,** 8293–8297 (1998).
2. K. Pervushin, A. Ono, C. Fernández, T. Szyperski, M. Kainosho, and K. Wüthrich, *Proc. Natl. Acad. Sci. USA* **95,** 14147–14151 (1998).
3. J. Wöhnert, A. J. Dingley, M. Stoldt, M. Göhlach, S. Grzesiek, and L. R. Brown, *Nucleic Acids Res.* **27,** 3104–3110 (1999).
4. A. Majumdar, A. Kettani, and E. Skripkin, *J. Biomol. NMR* **14,** 67–70 (1999).
5. A. Majumdar, A. Kettani, E. Skripkin, and D. J. Patel, *J. Biomol. NMR* **15,** 207–211 (1999).
6. M. Gueron, J. L. Leroy, and R. H. Griffey, *J. Am. Chem. Soc.* **105,** 7262–7266 (1983).
7. M. Goldman, *J. Magn. Reson.* **60,** 437–452 (1984).
8. K. Pervushin, R. Riek, G. Wider, and K. Wüthrich, *Proc. Natl. Acad. Sci. USA* **94,** 12366–12371 (1997).
9. G. Zhu, X. Kong, X. Yan, and K. Sze, *Angew. Chem., Int. Ed.* **37,** 2859–2861 (1998).
10. A. J. Dingley, J. E. Masse, R. D. Peterson, M. Barfield, J. Feigon, and S. Grzesiek, *J. Am. Chem. Soc.* **121,** 6019–6027 (1999).
11. K. Pervushin, C. Fernández, R. Riek, A. Ono, M. Kainosho, and K. Wüthrich, *J. Biomol. NMR.* **16,** 39–46 (2000).
12. A. Meissner and O. W. Sørenson, *J. Magn. Reson.* **143,** 387–390 (2000).
13. F. Cordier, A. J. Dingley, and S. Grzesiek, *J. Biomol. NMR* **13,** 175–180 (1999).
14. K. Pervushin, G. Wider, and K. Wuthrich, *J. Biomol. NMR* **12,** 345–348 (1998).
15. V.Sklenar, *J. Magn. Reson. A.* **114,** 132–153 (1995).
16. M. Piotto, V. Saudek, and V. Sklenár, *J. Biomol. NMR* **2,** 661–665 (1992).
17. X. Yan, H. Xue, H. Liu, J. Hang, J. T.-F. Wong, and G. Zhu, *J. Biol. Chem.* **275,** 6712–6716 (2000).
18. A. Bax, M. Ikura, L. E. Kay, and G. Zhu, *J. Magn. Reson.* **91,** 174–178 (1991).
19. G. Zhu, D. A. Torchia, and A. Bax, *J. Magn. Reson. A* **105,** 219–222 (1993).
20. K. L. Anderson-Altmann, C. G. Phung, S. Mavromoustakos, Z. Zheng, J. C. Facelli, C. D. Poulter, and D. M. Grant, *J. Phys. Chem.* **99,** 10454–10458 (1995).
21. G. Cornilescu, B. E. Ramirez, M. K. Frank, G. M. Clore, A. M. Gronenborn, and A. Bax, *J. Am. Chem. Soc.* **121,** 6275–6279 (1999).